Sustainable Energy & Fuels

ROYAL SOCIETY OF CHEMISTRY

COMMUNICATION

View Article Online
View Journal | View Issue

Cite this: *Sustainable Energy Fuels*, 2025, **9**, 5832

Received 14th May 2025
Accepted 7th September 2025

DOI: 10.1039/d5se00687b

rsc.li/sustainable-energy

Sodium-ion battery research @ BAM (I): investigating the thermal runaway behaviour of commercial sodium-ion battery cells

Nils Böttcher, Luise Sander, Alexander Ulbricht, Martinus Putra Widjaja, Tim-Patrick Fellinger, Anita Schmidt and Jonas Krug von Nidda *

Commercially available sodium-ion battery (SIB) cells, with energy densities comparable to lithium-ion battery (LIB) cells based on $LiFePO_4$, were investigated regarding their safety behaviour under thermal abuse conditions. Tests were carried out in an inert atmosphere. The SIB-cells went into thermal runaway (TR), intriguingly, even at a rather low state of charge of 30%. The TR-event was coupled with a pronounced jelly roll ejection, challenging the interpretation of the TR-diagrams. These findings highlight the necessity of incorporating SIB-cells into the ongoing safety classification discussions for LIB-cells.

Introduction

Sodium-ion batteries (SIBs) are a promising alternative and complementary technology to lithium-ion batteries (LIBs).[1] SIBs are especially promising for stationary applications, however, are also discussed for use in power tools and even electric vehicles.[2] Compared to LIBs, active materials of SIBs generally are more abundant and more geographically evenly distributed.[3] For approximately the past two years, the first SIB-cells have been accessible to private consumers in Europe, reflecting their increasing availability in the private sector. State-of-the-art SIB-cells reach energy densities of *ca.* 150 Wh kg^{-1}, approaching the values of LIBs based on lithium iron phosphate ($LiFePO_4$, LFP) cathode technology. The second generation of commercial SIB-cells of BYD (Naxtra battery), which is supposed to be produced in series from December 2025 on, apparently reaches 175 Wh kg^{-1}.[4] Next to energy density and lifetime, one very important aspect is the safety of battery cells. SIBs are generally discussed to be safer than existing LIBs due to their lower full-cell voltage and smaller energy densities, as observed for some of the first prototype SIB-cells.[5–9] However, as development aims for higher energy densities, an important question arises: how safe are the currently available commercial SIB-cells?

Coinciding with the availability of SIB-cells for private customers, several articles have been published analysing their electrochemical properties, as well as the electrodes and materials used in these cells.[10–13] Regarding safety testing, LIB-research has shown that the chosen abuse method can significantly influence the test outcome.[14–16] Furthermore, the safety behaviour of aged LIB-cells can differ substantially from the results of begin-of-life cells depending on the ageing path.[17–21] Currently, the Informal Working Group (IWG) of the Sub-Committee of Experts on the Transport of Dangerous Goods (TDG) of the United Nations (UN) develops a hazard based classification system for batteries to be included in the UN-Recommendations for the transport of dangerous goods.[22–24] In addition to developing the classification scheme, thermal abuse test protocols are developed providing the experimental criteria for this classification of cells and batteries.

To date, only a limited number of studies have investigated the safety of currently available SIB-cells. Bordes *et al.* assessed the vent gas of SIB-cells with $Na_3V_2(PO_4)_2F_3$ (NVPF) cathodes, concluding that – in a simplified manner – the specific cell type investigated showed similarities with LFP-cells in terms of the nature and quantity of emitted gas.[25] Like for LIBs, one of the main challenges in drawing a general conclusion about "the one" safety of commercial SIB-cells is their wide variety in active materials and electrolytes. Especially, the cathode materials differ quite a lot. The main classes are Prussian blue analogues, layer oxide materials (*e.g.*, $NaNi_{0.33}Fe_{0.33}Mn_{0.33}O_2$ (NFMO)) and polyanion materials (*e.g.*, NVPF), which show very different behaviour under thermal stress. Hence, it is not surprising that SIB-cells comprising different cathode materials show different properties during accelerated rate calorimetry (ARC) studies, which was shown in the very recent work of Carter *et al.*[26]

The present study reports the behaviour of commercial 18650 SIB-cells upon thermal abuse in a nitrogen (N_2) atmosphere, as a function of their state of charge (SOC). The results are analysed regarding the occurrence of a thermal runaway

Bundesanstalt für Materialforschung und -prüfung (BAM), Unter Den Eichen 87, 12205 Berlin, Germany. E-mail: jonas.krug-von-nidda@bam.de

(TR), the temperature of TR-onset, the maximum cell temperature and the maximum overpressure inside the test chamber. Moreover, the determined values are compared to the SOC-dependent behaviour of LFP-based 18650 LIB-cells with a similar capacity. At full SOC, the SIB-cells demonstrated a comparable behaviour to the LFP-cells with regard to the majority of the analysed TR-parameters, however, causing clearly larger overpressures. At a rather low SOC of 30%, the SIB-cell exhibited a mild TR during thermal abuse, whereas the LFP-cell showed no detectable rapid increase in temperature, even up to a cell temperature of 350 °C. In general, the herein studied SIB-cell type showed a very strong tendency towards jelly roll ejection, even though the cell holder tightly surrounded the cell on all sides and was covered by a lid. Hence, TR-identification based on only the cell's surface temperature may lead to misleading interpretations. Overall, the results show the importance of establishing suitable abuse test protocols applicable also for SIBs and to include SIB-cells in the planned hazard-based classification system to complement the existing minimum requirements for LIBs and SIBs in the international dangerous goods regulations and the respective 38.3 tests in the UN Manual of tests and criteria.[27]

Results and discussion

Cell type characterization and description of tests

Prior to the abuse test, one of the commercial SIB-cells was disassembled and analyzed by scanning electron microscopy (SEM) and energy-dispersive X-ray spectroscopy (EDX) to gain further safety-relevant information based on the active material composition of the cell (Fig. S1, SI). According to the EDX-measurements, the composition of the cathode active material is $Na_xNi_{0.33}Fe_{0.33}Mn_{0.33}O_2$, pointing to the layered sodium nickel iron manganese oxide (NFMO111). As revealed by SEM analysis, the anode consists of irregularly shaped particles with a broad size distribution, ranging from approximately 1 to 12 μm in diameter, that appear to be fragments of a milling process. Considering the particle size and shape, it can be speculated to be a biomass based hard carbon (HC) material, similar to the commercially available KURANODE® by Kuraray. According to the work of Sander *et al.*, conducting a multiscale analysis of a very similar 18650 SIB-cell from the same supplier, it can be assumed that the electrolyte is a mixture of organic carbonates.[28] The active material's basis is reminiscent of common LIBs (carbonaceous anode, layered metal oxide cathode and organic carbonate electrolyte), therefore no specifically adjusted risk assessment was needed for the abuse tests of this SIB cell type.

As noted, current SIB-cells offer energy densities comparable to LFP-based LIBs. Given that the nominal energy density often indicates thermal event severity, commercial LFP-cells with similar values were used as safety test references. The properties of both cell types are summarized in Table 1.

The received SIB-cells were stored at 8 ± 2 °C to minimize the influence of calendric ageing on the safety performance. Prior to safety testing, all cells were pre-cycled applying the standard conditions given in the respective data sheet, to assure that the tested cells are no production outliers. The respective values are given in Table S1, SI. Based on the last full discharge cycle, the cell-specific capacity (C_{cell}) and energy (E_{cell}) at 100% SOC were determined. This C_{cell}-value was also used to determine the discharge time to reach – if required – an SOC below 100% for the abuse test.

Abuse testing was performed in a self-designed, pressure tight test chamber (Fig. S2, SI). The details of the test setup are described by Böttcher *et al.*[29] Briefly, the cell was placed in a heat-insulated holder with a lid, and all tests were conducted under N_2-atmosphere to prevent combustion of emitted gases. The occurrence of combustion largely depends on oxygen levels, and significantly influences the maximum overpressure (p_{max}) observed during a TR.[29] During the abuse test, the cell was heated by a heating cartridge on one side with a constant heating rate of 15 K min^{-1} until a TR occurred or until the cell temperature (T_{cell}) surpassed 250 °C. Synchronously with T_{cell}, the cell voltage (U_{cell}), and the overpressure inside the test chamber (p) were recorded. The test setup and protocol were chosen in accordance with the discussions in the laboratory testing group of the IWG-TDG. More detailed information about the setup can be found in the SI.

Three SOCs were selected for safety tests of the SIB-cells: (i) 100% SOC, representing the worst-case scenario, (ii) 70% SOC, representing an intermediate state of charge, *e.g.*, a typical SOC in operation, and (iii) 30% SOC, representing the allowed maximum SOC of LIB- and SIB-cells as cargo in air transport, according to the Dangerous Goods Regulation of the International Air Transport Association/International Civil Aviation

Table 1 Summary of cell-characteristics of the SIB- and LIB-cells investigated

Parameter	SIB-cell	LIB-cell
Manufacturer	Shenzhen Zhonghuajia Technology Co., Ltd	Heter Electronics Group Co., Ltd
Model	SIB-18650-1300 mAh	HTCF18650-1600 mAh-3.2V
Cell format	18650	18650
Standard capacity	1300 mAh	1600 mAh
Nominal voltage	3.0 V	3.2 V
Cell weight	40 +/− 2g	42 g
Specific energy density	97.5 Wh kg^{-1}	122 Wh kg^{-1}
Cathode active material	$NaNi_{0.33}Fe_{0.33}Mn_{0.33}O_2$ (NFMO111)	$LiFePO_4$ (LFP)
Anode active material	Hard carbon (HC)	Graphite
Main electrolyte components	Based on organic carbonates (inferred from ref. 28)	Not analyzed

Organization Technical Instructions (IATA/ICAO-TI).[30] For the reference LIB-cell, only the two boundaries, thus 30% SOC and 100% SOC, were chosen.

SOC-dependent abuse behaviour of SIB-cells *vs.* LIB-cells

The trend in T_{cell}, U_{cell}, and p_{max} of the SIB-cells at various SOCs are depicted in Fig. 1. At a certain cell temperature, all cells showed a very large drop in U_{cell} during the test. This temperature is herein discussed as $T_{volt\text{-}drop}$. Apparently, a lower U_{cell} – thus, a lower SOC – leads to an increased $T_{volt\text{-}drop}$. For an SOC of 100%, 70% and 30% the drop in cell voltage occurs at 79 °C, 88 °C and 103 °C, respectively.

Intriguingly, the trend of the maximum value of T_{cell} during the test, defined as $T_{TR,max}$, with respect to the SOC is counterintuitive, showing values of 182 °C, 227 °C and 295 °C with decreasing SOC from 100%, *via* 70% to 30%. An interpretation of the fully charged SIB-cell based on the TR-diagram only would indicate the absence of a TR, because of the observed low $T_{TR,max}$ and the absence of a jump-like increase in T_{cell}. However, a video recorded during the actual test showed a rather strong TR-reaction of this sample. Visual inspection of the cells after TR revealed, that the tested SIB-cells show a very strong tendency of jelly roll ejection, being more severe for larger SOCs (see Fig. 1c–h and S3a–c, SI). At 100% SOC, the jelly roll ejection appears to occur rapidly, causing an immediate drop in the cell can's surface temperature where the temperature sensor was placed. Notably, this ejection occurred in the presence of a lid on the cell holder, which had previously been sufficient to prevent jelly roll ejection in a wide range of tested LIB-cell types.[29] At 30% SOC, the jelly roll remained inside the cell can, indicating a valid determination of $T_{TR,max}$. Interestingly, the same trend of SOC-dependent jelly roll ejection was also observed when repeating the tests under air-atmosphere (see Fig. S3d–e, SI).

Next to T_{cell}, the overpressure trend inside the test chamber can disclose useful information regarding the TR (see Fig. 1b).[31] For all three cells, the chamber remained at ambient pressure until a jump-like development of overpressure occurred. This can be connected to the occurrence of a TR-event. Since the tests were carried out under closed conditions, p stabilized, after the significant increase during the TR, at a relatively constant value. As jelly roll ejection leads to misinterpretation when choosing T_{cell} to determine the TR-onset temperature ($T_{TR,onset}$), the temperature at which the change in pressure (Δp-rate) exceeded 3 mbar s^{-1} was defined as $T_{TR,onset}$ in this study. This identification parameter reveals that with decreasing SOC, the $T_{TR,onset}$ increases from 182 °C, to 193 °C and finally to 218 °C. It should be noted that for samples with lower SOCs, the heating rate commonly used in literature (*e.g.*, 3 K min^{-1}) can also be applied for determining the $T_{TR,onset}$. The resulting values, 194 °C for an SOC of 70% and 214 °C for an SOC of 30%, differ only slightly from those based on the Δp-rate. Hence, the $T_{TR,onset}$ values reported herein, based on the Δp-rate, can be considered reliable. Moreover, larger SOCs lead to a higher p_{max} value, *i.e.*, 6 mbar, 90 mbar and 111 mbar for an SOC of 30%, 70% and 100%, respectively.

Generally, the SOC trend is in line with literature results for LIB-cells, showing a more severe TR, as indicated by larger p_{max}, and a lower $T_{TR,onset}$, for larger SOCs.[29,32–34] Furthermore, this trend aligns with recent findings by Carter *et al.*, who used ARC to study the safety of various commercial SIB-cell types.[26] Intriguingly, their results revealed that one of their NFMO-

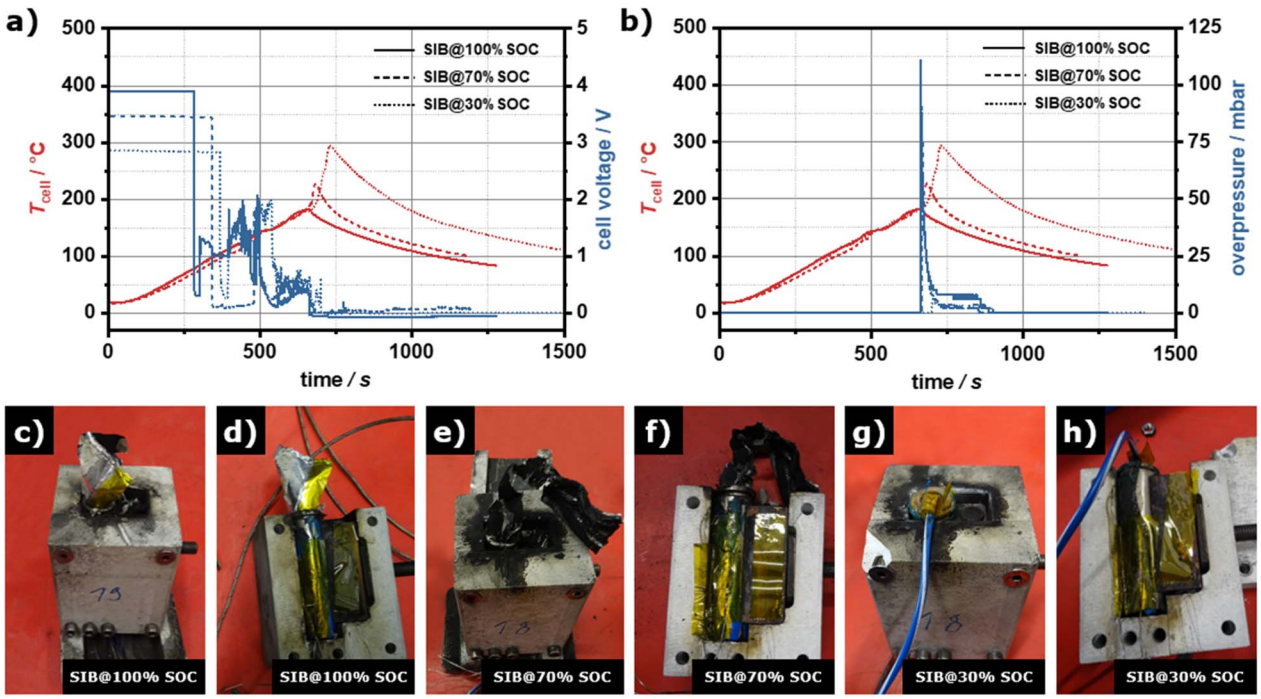

Fig. 1 Trends of (a) cell temperature (T_{cell}) and cell voltage (U_{cell}), and (b) T_{cell} and overpressure (p) during the thermal abuse test of the SIB-cells at different SOCs. Photographs of the SIB-cells after the thermal abuse test at (c and d) 100% SOC, (e and f) 70% SOC and (g and h) 30% SOC.

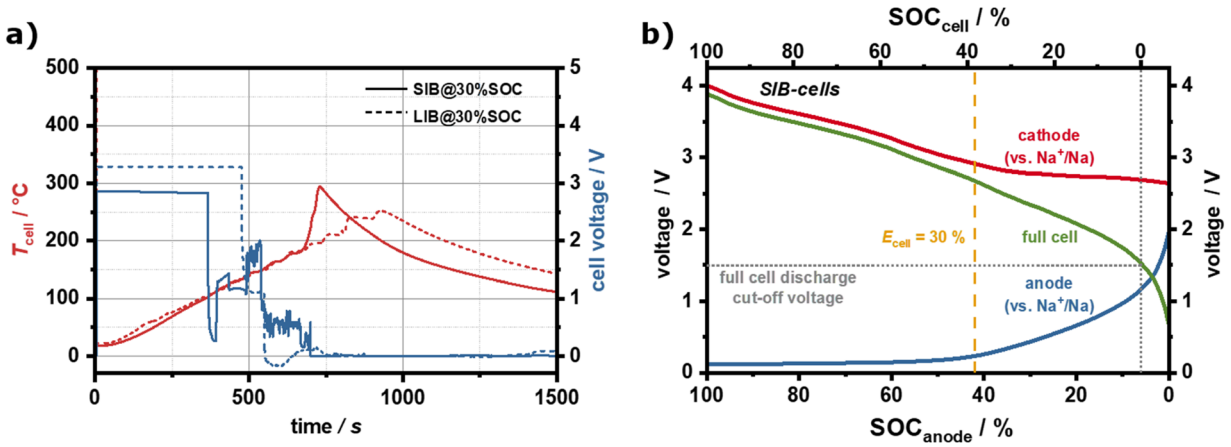

Fig. 2 (a) Trends in cell temperature (T_{cell}) and cell voltage (U_{cell}) for both the SIB- and the LIB-cell, each at an SOC of 30%. (b) Theoretical full cell voltage profile of an SIB, based on the respective half cell curves from the data provided for commercially available HC electrode sheets and NFMO-material in ref. 36 and 37, respectively ($n:p$-ratio = 1.5 : 1, assumed initial coulomb efficiency of anode = 90%).

based SIB cell types exhibited a TR-onset even at very low SOCs, *i.e.*, 25% and 0%. Notably, the onset temperatures determined by Carter *et al.*, being in the range of 86 °C to 91 °C, are significantly lower than the $T_{TR\text{-}onset}$ identified here, which may be related to experimental differences between ARC-tests and the herein used thermal abuse setup.[15] Furthermore, the characteristics of the ARC test, *e.g.*, a rather slow stepwise heating, likely mitigated jelly roll ejection of this NFMO-cell type, enabling the determination of peak temperatures ranging from 275 °C to 442 °C for SOCs between 0% and 100%. A deeper understanding of the mechanisms behind jelly roll ejection is of high interest and should be addressed in future work.

Comparing the trends of T_{cell} and U_{cell} for the SIB-cell and the reference LIB-cell at the lowest SOC of 30% reveals that the LIB-cell does not show a significant increase in self-heating up to the maximum temperature of 250 °C (see Fig. 2a and also S4, SI). Moreover, the U_{cell}-drop of the LIB-cell occurs at a higher temperature, *i.e.*, $T_{volt\text{-}drop}$ states 133 °C and 103 °C for the LIB- and SIB-cell, respectively. The visible inspection confirms the rather undamaged state of the LIB-cell after the abuse test (Fig. S4e–g, SI). To confirm that increasing the maximum temperature did not affect the test outcome, an additional test was conducted at a maximum temperature of 350 °C. However, no TR was detected in the respective test for the LIB-cell at 30% SOC (see Fig. S5, SI). It should be noted that at 30% SOC, the LIB-cell still has a significantly higher E_{cell} than the SIB-cell, with values of 1.44 Wh and 0.89 Wh, respectively (*cf.* Table S1, SI). At an SOC of 100%, the LFP-cell does show a clear TR, with a $T_{TR,onset}$, $T_{TR,max}$, and p_{max} of 264 °C, 359 °C, and 11 mbar, respectively (see Fig. S4a and b, SI). In contrast to the SIB-cell, no jelly roll ejection occurred for the LIB-cell, even at 100% SOC (see Fig. S4c and d, SI).

Discussion of intrinsic SOC differences of SIBs *vs.* LIBs

Based on the intuitive assumption that the SOC is directly connected to the energy content of the cell, it is surprising that a SIB-cell shows a TR at a rather low SOC of 30%, and even at 0% during an ARC test.[26] However, the relation between the energy content and the SOC is not that trivial and differs between LIBs and SIBs significantly. The main reason for this is that the anode potential curve differs notably between HC – typically used in SIBs – and graphite – commonly used in LIBs. The crystalline nature of graphite results in a rather flat potential profile over the entire SOC range, as depicted in Fig. S6, SI.[35] Hence, almost no lithium is left inside the graphite anode when the full cell cut-off voltage is approached during discharge. A full cell voltage plot, calculated based on the respective half cell curves, illustrates this phenomenon (as depicted in Fig. S6, SI).[35] Expressed differently, the SOC of the full cell (SOC_{cell}) nicely mimics the SOC of the anode (SOC_{anode}) for an LFP-based LIB-cell with a graphite anode. In exact terms, SOC_{anode} states *ca.* 0.8% at an SOC_{cell} of 0%, taking half cell curves from literature and assuming a $n:p$-ration of 1.1 : 1.[35]

Contrarily, the substantially sloping capacity profile of HC-materials – due to the non-crystalline nature of HCs – results in remaining sodium within the anode at the discharge cut-off voltage of the SIB full cell (see Fig. 2b). The half cell profiles for the anode and cathode are extracted from the data sheets of commercial HC electrode sheets and NFMO-material, respectively.[36,37] Assuming an $n:p$-ratio of 1.5 : 1, based on the analysis of a very similar cell in the work of Sander *et al.*, SOC_{anode} still states *ca.* 6% when SOC_{cell} = 0% (see Fig. 2b).[28] This effect would even be more pronounced for pre-sodiated systems.

Furthermore, for SIB-cells it must be considered that a sloping anode also causes a pronounced shift in energy *vs.* capacity content. More precisely, an E_{cell} of 30% translates into and SOC_{cell} of *ca.* 38% and an SOC_{anode} of *ca.* 42% for an SIB-cell. On the contrary, for an LFP-cell, 30% E_{cell} converts to an SOC_{cell} and SOC_{anode} of *ca.* 30% and *ca.* 31%, respectively.

The trends of $T_{TR,onset}$, $T_{TR,max}$ and p_{max} of all cells discussed herein are summarized in Fig. 3. Compared to the LIB-cell at 100% SOC, the fully charged SIB-cell evidently showed a lower $T_{TR\text{-}onset}$ (182 °C *vs.* 264 °C) and larger p_{max} (111 mbar *vs.* 11 mbar). This data indicate that the SIB-cell tested herein is less safe than the LIB-cell chosen for comparison. It should be noted that normalizing with respect to energy content would further

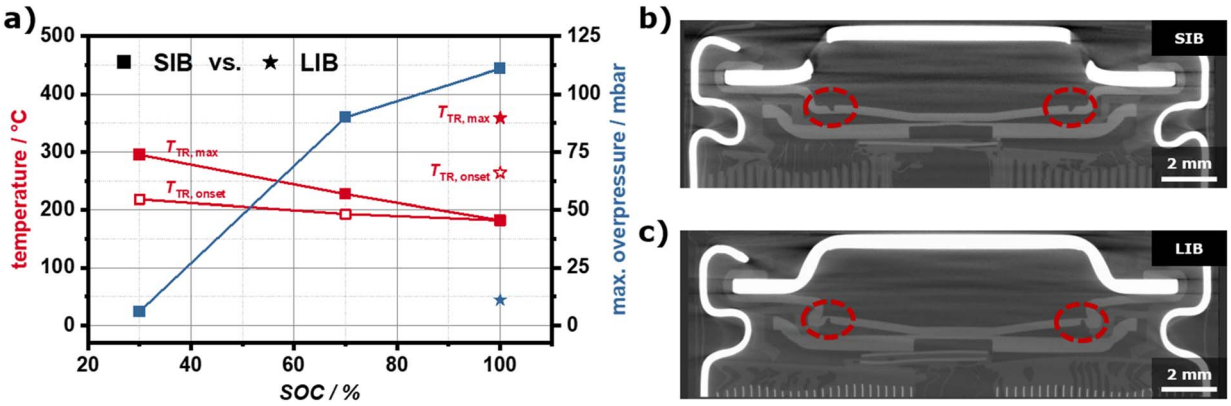

Fig. 3 (a) Summary of the SOC-dependent TR-behaviour, by means of $T_{TR,onset}$, $T_{TR,max}$ and p_{max} of the SIB- and LIB-cells investigated. The $T_{TR,max}$-values of the SIB-cells at 70% SOC and 100% SOC are not reasonable due to the strong jelly roll ejection at these SOCs. CT-images of the top of (b) the SIB-cell and (c) the LIB-cell.

emphasize the lower safety of the SIB cell, given its lower energy content, *e.g.*, 3.65 Wh for the fully charged SIB-cell compared to 4.86 Wh for the fully charged LIB-cell. However, other SIB cell types may behave differently. Moreover, next to the behavior of one single cell upon abuse, the occurrence of a TR-propagation from cell to cell is of utmost importance for safety ratings. In this respect, it may even be possible that a controlled jelly roll ejection could help prevent TR-propagation and thereby increase safety, provided the ejected material can be intentionally directed away from other cells.

The cause of the very severe jelly roll ejection observed for the SIB-cells is of particular interest. As known from Carter *et al.*, cells with different SIB cathode materials, behave quite differently during ARC-tests.[26] Furthermore, an NFMO cathode, being a layered oxide type, is expected to show stronger TR-effects than an LFP cathode – potentially even resembling, to some extent, the behaviour of layered oxide cathodes in LIBs. This is consistent with the comparison between $LiCoO_2$, $Li(Ni_xMn_yCo_z)O_2$ as well as $LiNi_xCo_yAl_zO_2$ (all layered oxides) and LFP, a polyanion, in LIBs.[29] A further explanation may be found in the difference in manufacturing of the two cell types. Intriguingly, in-house X-ray computed tomography (CT) studies of the two cell types revealed that the predetermined breaking point of the venting cap is quite differently designed (see Fig. 3b and c). Whereas the venting cap of the SIB cell is carved on its top surface, the venting cap of the LIB is carved on its bottom surface. It is possibly that this difference causes rupturing at a higher cell internal pressure of the SIB-cell, exacerbating TR-effects.[38] Nonetheless, the high tendency for jelly roll ejection could be still attributed to other factors, such as the solely use of aluminum current collectors in the SIB-cell, which can melt at relatively low local temperatures compared to the anodic copper current collector in LIB-cells, potentially influencing the speed of cell internal TR-propagation.

It is important to note though, that the presented safety behavior is of course only valid for the specific SIB-cell type, and even the specific manufacturing batch, investigated herein. Moreover, it should be recognized that SIB- offer distinct advantages over LIB-cells in terms of resource availability, sustainability, and reduced cost and weight, due to the solely use of aluminum current collectors. This design prospectively allows for reversible discharge to 0 V without irreversible damage, unlike LIB-cells, whose anodic copper current collectors may corrode at low voltages.[39] As a result, SIB-cells can potentially be stored and transported safely at 0 V, posing no risk of energy release even if severely damaged. However, storage at 0 V may impair cycling performance, highlighting the need for further research on SEI-stabilization or reactivation strategies.[40,41]

Conclusions

In summary, the present study reveals that current commercial SIB-cells must be classified alongside LFP-cells in terms of their safety behavior as they can even undergo TR at a rather low SOC of 30%. This is herein connected to the discrepancy between the SOC on cell level and the SOC on anode level – a difference that is more pronounced in SIBs due to the extended sloping region in the voltage profile of HC-anodes. Hence, even at an SOC_{cell} of 0%, the SOC_{anode} states *ca.* 6%, indicating that there is still Na stored inside the SIB-anode. At high SOCs, the TR event in the tested SIB cell type was accompanied by pronounced jelly roll ejection, complicating TR-identification based on cell temperature alone. Understanding the underlying mechanisms warrants further investigations.

Overall, the results clearly show that the wide-spread assumption that SIB-cells are generally safer than LIB-cells is oversimplified. Hence, it is important to incorporate SIB-cells into the ongoing safety classification discussions for LIB-cells, allowing their transport and thereby market access. At the same time the early stages of large-scale commercial SIB-cell manufacturing present an opportunity to further optimize passive safety features and material components to increase SIB-safety in the future.

Author contributions

Nils Böttcher: writing – original draft, investigation, visualization, methodology, formal analysis, software; Luise Sander:

resources, investigation, writing – review & editing; Alexander Ulbricht; resources, investigation, writing – review & editing; Martinus Putra Widjaja: resources, investigation, writing – review & editing; Tim-Patrick Fellinger: supervision, writing – review & editing; Anita Schmidt: conceptualization, funding acquisition, project administration, writing – review & editing; Jonas Krug von Nidda: writing – original draft, conceptualization, methodology, supervision, project administration.

Conflicts of interest

There are no conflicts to declare.

Data availability

Any data that support the finding of this study are included within the article or as a part of the SI. See DOI: **https://doi.org/10.1039/d5se00687b**.

Acknowledgements

M. Setzchen, O. Zeh, F. Plath, and L. Petersen (all BAM) are acknowledged for their help with the practical execution of the abuse tests. R. Leonhardt and H. Markötter (both BAM) are greatly acknowledged for the post-processing of images and (especially) CT-related discussions, respectively. T. Lange and V.-D. Hodoroaba (both BAM) are greatly acknowledged for the general help with the SEM-measurements and for providing the measurement capabilities of the FlexSEM, respectively. This work was financially supported by BMV as part of the LiKlas-project.

References

1 A. Rudola, R. Sayers, C. J. Wright and J. Barker, *Nat. Energy*, 2023, **8**, 215–218.
2 K. M. Abraham, *ACS Energy Lett.*, 2020, **5**, 3544–3547.
3 C. Vaalma, D. Buchholz, M. Weil and S. Passerini, *Nat. Rev. Mater.*, 2018, **3**, 18013.
4 CATL, *Naxtra Battery Breakthrough & Dual-Power Architecture: CATL Pioneers the Multi-Power Era*, accessed 09.05.2025, **https://www.catl.com/en/news/6401.html**.
5 Q. Zhou, Y. Li, F. Tang, K. Li, X. Rong, Y. Lu, L. Chen and Y.-S. Hu, *Chin. Phys. Lett.*, 2021, **38**, 076501.
6 Y. Li, Y.-S. Hu, X. Qi, X. Rong, H. Li, X. Huang and L. Chen, *Energy Storage Mater.*, 2016, **5**, 191–197.
7 R. Usiskin, Y. Lu, J. Popovic, M. Law, P. Balaya, Y.-S. Hu and J. Maier, *Nat. Rev. Mater.*, 2021, **6**, 1020–1035.
8 A. Rudola, A. J. R. Rennie, R. Heap, S. S. Meysami, A. Lowbridge, F. Mazzali, R. Sayers, C. J. Wright and J. Barker, *J. Mater. Chem. A*, 2021, **9**, 8279–8302.
9 K. Chayambuka, G. Mulder, D. L. Danilov and P. H. L. Notten, *Adv. Energy Mater.*, 2020, **10**, 2001310.
10 K. Bischof, V. Marangon, M. Kasper, A. Aracil Regalado, M. Wohlfahrt-Mehrens, M. Hölzle, D. Bresser and T. Waldmann, *J. Power Sources Adv.*, 2024, **27**, 100148.
11 V. Marangon, K. Bischof, A. A. Regalado, M. Keppeler, M. Pogosova, M. Wan, J. Choi, S. Fleischmann, T. Diemant, M. Wohlfahrt-Mehrens, M. Hölzle, T. Waldmann and D. Bresser, *J. Power Sources*, 2025, **634**, 236496.
12 H. Laufen, S. Klick, H. Ditler, K. L. Quade, A. Mikitisin, A. Blömeke, M. Schütte, D. Wasylowski, M. Sonnet, L. Henrich, A. Schwedt, G. Stahl, F. Ringbeck, J. Mayer and D. U. Sauer, *Cell Rep. Phys. Sci.*, 2024, **5**, 101945.
13 M. He, R. Davis, D. Chartouni, M. Johnson, M. Abplanalp, P. Troendle and R.-P. Suetterlin, *J. Power Sources*, 2022, **548**, 232036.
14 W. Q. Walker, K. Cooper, P. Hughes, I. Doemling, M. Akhnoukh, S. Taylor, J. Darst, J. Billman, M. Sharp, D. Petrushenko, R. Owen, M. Pham, T. Heenan, A. Rack, O. Magdsyuk, T. Connolley, D. Brett, P. Shearing, D. Finegan and E. Darcy, *J. Power Sources*, 2022, **524**, 230645.
15 T. Rappsilber, N. Yusfi, S. Krüger, S.-K. Hahn, T.-P. Fellinger, J. Krug von Nidda and R. Tschirschwitz, *J. Energy Storage*, 2023, **60**, 106579.
16 C. Essl, A. W. Golubkov and A. Fuchs, *J. Electrochem. Soc.*, 2020, **167**, 130542.
17 T. Waldmann, M. Wilka, M. Kasper, M. Fleischhammer and M. Wohlfahrt-Mehrens, *J. Power Sources*, 2014, **262**, 129–135.
18 A. Friesen, F. Horsthemke, X. Mönnighoff, G. Brunklaus, R. Krafft, M. Börner, T. Risthaus, M. Winter and F. M. Schappacher, *J. Power Sources*, 2016, **334**, 1–11.
19 M. Börner, A. Friesen, M. Grützke, Y. P. Stenzel, G. Brunklaus, J. Haetge, S. Nowak, F. M. Schappacher and M. Winter, *J. Power Sources*, 2017, **342**, 382–392.
20 Y. Jia, X. Gao, L. Ma and J. Xu, *Adv. Energy Mater.*, 2023, **13**, 2300368.
21 Y. Preger, L. Torres-Castro, T. Rauhala and J. Jeevarajan, *J. Electrochem. Soc.*, 2022, **169**, 030507.
22 Informal Document on the Hazard-Based Classification of Lithium Batteries and Cells, 06/2023, Informal Working Group of the Sub–Committee of Experts on the Transport of Dangerous Goods, UN–SCETDG–62–INF14e.
23 United Nations, *Recommendations on the Transport of Dangerous Goods*, Model Regulations, 23rd edn, 2023, vol. **I**.
24 Informal Document on the Hazard-Based Classification of Lithium Batteries and Cells 04/2025, Informal Working Group of the Sub–Committee of Experts on the Transport of Dangerous Goods, UN/SCETDG/66/INF.12.
25 A. Bordes, G. Marlair, A. Zantman, A. Chesnaye, P.-A. L. Lore and A. Lecocq, *ACS Energy Lett.*, 2022, **7**, 3386–3391.
26 R. Carter, G. H. Waller, C. Jacob, D. Hayman, P. J. West and C. T. Love, *Energies*, 2025, **18**, 661.
27 *UNITED NATIONS - Manual of Tests and Criteria*, 2023, 8th edn, ST/SG/AC.10/Rev.18.
28 L. Sander *et al.*, Sodium-Ion Battery Research at BAM (II): Linking Material and Electrode Properties to the Performance of Commercially Available Sodium-Ion Cells, 2025, to be submitted.
29 N. Böttcher, N. Yusfi, J. Kowal, A. Schmidt and J. Krug von Nidda, Linking Key Features of Commercial Lithium Ion

Cells to Thermal Runaway Effects, 2025, under review, DOI: 10.2139/ssrn.5229771.
30 *ICAO Technical Instructions for the Safe Transport of Dangerous Goods by Air*, Doc 9284, 03/2025, pp. 2025–2026.
31 B. Mao, C. Fear, H. Chen, H. Zhou, C. Zhao, P. P. Mukherjee, J. Sun and Q. Wang, *eTransportation*, 2023, **15**, 100212.
32 K. C. Abbott, J. E. H. Buston, J. Gill, S. L. Goddard, D. Howard, G. E. Howard, E. Read and R. C. E. Williams, *J. Energy Storage*, 2023, **65**, 107293.
33 E. P. Roth, *ECS Trans.*, 2008, **11**, 19.
34 Q. Zhang, J. Niu, Z. Zhao and Q. Wang, *J. Energy Storage*, 2022, **45**, 103759.
35 B. Rowden and N. Garcia-Araez, *Energy Rep.*, 2021, **7**, 97–103.
36 MTI-Corporation, *Data Sheet of Hard Carbon Single-Side Coated Al Foil for Sodium Ion Battery Anode (bcaf-BHCss)*, accessed 20.03.2025, https://mtixtl.com/products/hard-carbon-single-side-coated-al-foil-for-sodium-ion-battery-anode-241-l-x-200-w-x-240-209-thickness-mm-245-sheets-bag-bcaf-bhcss?_pos=241&_sid=242b249f243ae246d&_ss=r.
37 MTI-Corporation, *Data Sheet of Layered Oxide NaNi1/3Fe1/3Mn1/3O2 Powder for Sodium Ion Battery Cathode*, accessed 20.03.2025, https://mtixtl.com/products/sib-nfmo?_pos=2&_sid=49d92ab80&_ss=r.
38 H. Sun, G. Li, H. Zhao, Y. Yang and C. Yuan, *Energies*, 2025, **18**, 1173.
39 S. Dayani, H. Markötter, J. K. von Nidda, A. Schmidt and G. Bruno, *Adv. Mater. Technol.*, 2024, **9**, 2301246.
40 T. Song, B. Kishore, Y. Lakhdar, L. Chen, P. R. Slater and E. Kendrick, *Batteries*, 2024, **10**, 361.
41 P. Desai, J. Huang, D. Foix, J.-M. Tarascon and S. Mariyappan, *J. Power Sources*, 2022, **551**, 232177.

